ORIGINAL ARTICLE

Cytometry PART A
Journal of Quantitative Cell Science

MIFlowCyt

A Flow Cytometry-Based Assay for High-Throughput Detection and Quantification of Neutrophil Extracellular Traps in Mixed Cell Populations

Olga Zharkova,[1†] Sen Hee Tay,[2,3,4,5†] Hui Yin Lee,[5] Tripathi Shubhita,[2,5] Wei Yee Ong,[6] Aisha Lateef,[3,4] Paul Anthony MacAry,[2] Lina Hsiu Kim Lim,[1] John Edward Connolly,[6] Anna-Marie Fairhurst[2,5*]

[1]Department of Physiology, Yong Loo Lin School of Medicine, National University of Singapore Singapore

[2]Department of Microbiology and Immunology, Yong Loo Lin School of Medicine, National University of Singapore Singapore

[3]Department of Medicine, National University Health System Singapore

[4]Division of Rheumatology, Department of Medicine, National University Hospital, National University Health System Singapore

[5]Singapore Immunology Network, Agency for Science, Technology and Research (A*STAR) Singapore

[6]Institute for Molecular and Cellular Biology, Agency for Science, Technology and Research (A*STAR) Singapore

Received 23 May 2018; Revised 26 September 2018; Accepted 16 October 2018

Grant sponsor: Institute for Molecular and Cellular Biology; Grant sponsor: Singapore Immunology Network

Additional Supporting Information may be found in the online version of this article.

*Correspondence to: Anna-Marie Fairhurst, Singapore Immunology Network, Agency for Science, Technology and Research, 8A Biomedical Grove, #04-06 Immunos, Singapore 138648
Email: annamarie_fairhurst@immunol.a-star.edu.sg

Abstract

Neutrophil extracellular traps (NETs) are web-like structures composed of decondensed chromatin and antimicrobial proteins that are released into the extracellular space during microbial infections. This active cell death program is known as NETosis. To date, florescence microscopy is the widely accepted method for visualization and quantification of NETs. However, this method is subjective, time consuming and yields low numbers of analyzed polymorphonuclear cells (PMNs) per sample. Increasing interest has emerged on the identification of NETs using flow cytometry techniques. However, flow cytometry analysis of NETs requires particular precautions for sample preparation to obtain reproducible data. Herein, we describe a flow cytometry-based assay for high-throughput detection and quantification of NETosis in mixed cell populations. We used fluorescent-labeled antibodies against cell markers on PMNs together with a combination of nucleic acid stains to measure NETosis in whole blood (WB) and purified PMNs. Using plasma membrane-impermeable DNA-binding dye, SYTOX Orange (SO), we found that cell-appendant DNA of NETting PMNs were positive for SO and DAPI. The combination of optimally diluted antibody and nucleic acid dyes required no washing and yielded low background fluorescence. Significant correlations were found for NETosis from WB and purified PMNs. We then validated the assay by comparing with time-lapse live cell fluorescence microscopy and determined very good intraassay and interassay variances. The assay was then applied to a disease associated with NETosis, systemic lupus erythematosus (SLE). We examined PMA-induced NETosis in peripheral PMNs from SLE patients and controls and in bone marrow PMNs from multiple murine models. In summary, this assay is observer-independent and allows for rapid assessment of a large number of PMNs per sample. Use of this assay does not require sophisticated microscopic equipment like imaging flow cytometers and may be a starting point to analyze extracellular trap formation from immune cells other than PMNs.

Key terms

neutophils; extracellular traps; flow cytometry

Introduction

Neutrophils, also known as polymorphonuclear cells (PMNs), are the first and most numerous innate immune cells recruited to sites of infection (1). Elimination of pathogenic material is achieved through a number of processes that include phagocytosis and the generation of reactive oxygen species via respiratory burst (2). This is assisted by the release of microbicidal peptides from cytoplasmic granules. The life cycle of the neutrophil includes maturation in the bone marrow before release into the circulation (3). Clearance of senescent neutrophils is completed by the reticuloendothelial system (3). In the bone marrow granulocyte-macrophage progenitor cells

ISAC International Society for Advancement of Cytometry

†These authors contributed equally to this work.

This work was supported by core funding from the Singapore Immunology Network and Institute for Molecular and Cellular Biology (to A.-M.F. and J.E.C.).

Published online 14 December 2018 in Wiley Online Library (wileyonlinelibrary.com)

DOI: 10.1002/cyto.a.23672

give rise to pre-neutrophils which are a proliferative neutrophil precursor population. These then develop into immature neutrophils before differentiating into mature neutrophils (4). Neutrophils have a low level of gene expression but are equipped with proteins required to kill microbes by the time they reach the circulation (5). Neutrophil elastase (NE) and myeloperoxidase (MPO) are stored in the azurophilic granules of naïve neutrophils (6). NE is serine protease that is neutrophil-specific. It primarily degrades virulence factors and destroys bacteria (6). MPO catalyzes the oxidation of halide ions such as chloride in the presence of hydrogen peroxide, to generate hypochlorous acid and other reactive products that mediate antimicrobial action (7).

Over a decade ago, a new form of active cell death program in neutrophils was described and named NETosis (8,9). NETosis is morphologically different from other forms of cell death such as apoptosis or necrosis (10). Neutrophil activation by microbes and other stimuli promotes reactive oxygen species (ROS) generation and the action of NE and MPO after their translocation from the azurophilic granules to the nucleus (6). NE cleaves histones and stimulates chromatin decondensation in the nucleus (6). In the late stages of this process, MPO binds to chromatin to drive further decondensation and the release of mesh-like structures with a chromatin backbone with attached globular domains, termed neutrophil extracellular traps (NETs) (6,9). The locally elevated concentration of antimicrobial proteins (e.g., citrullinated histones, MPO and NE) trap and promote the clearance of bacteria, fungi, parasites and viruses by NETs (Fig. 1A) (2,9). This dependency on neutrophil-specific factors explains in part why extracellular trap (ET) formation is observed mainly in PMNs, which are the most efficient producers of ROS, primarily through NADPH oxidase-dependent pathways (6,11,12). While NETs have antimicrobial roles, they also contribute to autoimmune diseases such as systemic lupus erythematosus (SLE) (13). Defective NET degradation has been associated with increased risk of lupus nephritis, with NETs observed in the kidney biopsy of a SLE patient with impaired NET degradation (14).

As its original description has become apparent that in addition to nuclear DNA, mitochondrial DNA (mtDNA) could also be used by lymphocytes, monocytes, and PMNs to form ETs without induction of cell death (15,16). In addition, none of the proteins associated with NETs are present in B cell ETs (16). Hence, although ETs classically contain citrullinated histones, MPO and NE; their specific composition continues to be defined (17).

SYTOX Orange (SO) is an intercalating dye that has negligible intrinsic fluorescence but large fluorescence enhancement (~450-fold) upon binding to double-stranded DNA (18–20). Therefore, it stands to reason that cell-appendant NET DNA could be detected using flow cytometry with SO (21). In addition, SO does not cross the plasma membrane of

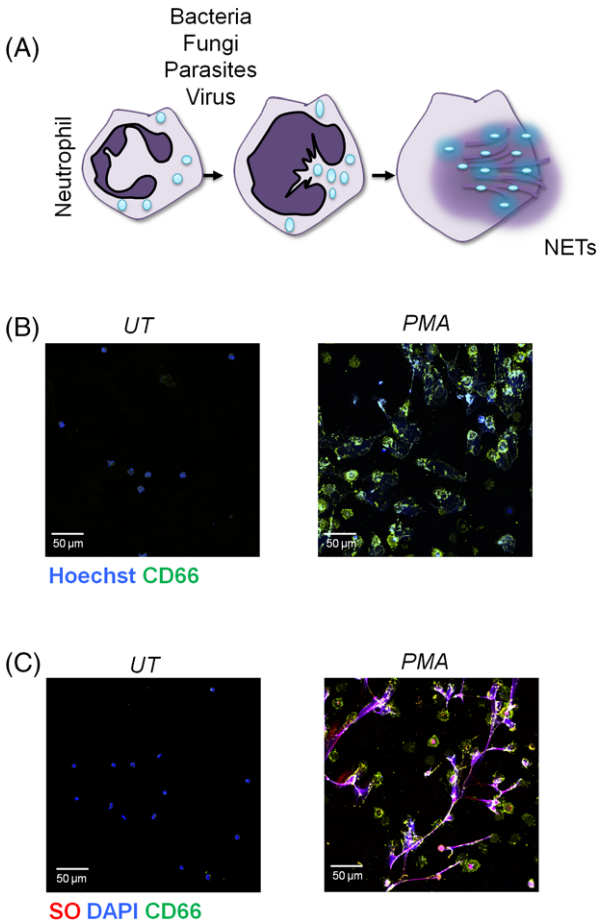

Figure 1. Visualizing NETosis on immunofluorescence confocal microscopy. (**A**) Schematic diagram representing a resting PMN undergoing activation and NET formation after encounter with pathogens. (**B**) Neutrophils were stained with anti-CD66-FITC and Hoechst. Surface expression of CD66 was upregulated following 30 nM PMA stimulation. (**C**) The long extended NET-DNA structures are clearly visible with SO and DAPI following 30 nM PMA treatment. Images were acquired using 40× oil objective on a Zeiss LSM800 confocal microscope.

live cells (20). There has been increasing interest for the identification of NETs utilizing flow cytometry techniques (22–25). However, flow cytometry analysis of NETs requires particular precautions for sample preparation to obtain reproducible data. In particular, this method should differentiate NETosis from other forms of cell death such as necrosis or apoptosis (21). In this report, we describe an optimized protocol utilizing a combination of SO and 4′,6-diamidino-2-phenylindole (DAPI) for two-color visualization of NETs on flow cytometry (20). SO^+DAPI^+ PMNs activated with phorbol 12-myristate 13-acetate (PMA) was dose- and time-dependent, as previously described (8,25). To verify that SO^+DAPI^+ PMNs were not due to other forms of cell death, we determined the following findings: (1) minimal SO^+DAPI^+ PMNs with epoptoside-induced apoptosis; (2) correlation in the percentage of SO^+DAPI^+ PMNs with NETosis rate obtained using time-lapse live cell microscopy; and (3) colocalization of extracellular DNA and NE on flow cytometry. Last, this flow cytometric-based assay can be used for both human and murine samples, including purified PMNs or mixed cell populations extracted from whole blood (WB) or bone marrow (BM). In addition, this is the first flow cytometry assay, which does not require purification as isolation procedures may activate the PMNs (22,24–26).

Materials and Methods

Subjects

Patients with SLE attending the outpatient clinics of National University Hospital who fulfilled at least four of the revised American College of Rheumatology revised classification criteria or healthy donors (HD) were invited to take part in the study (27). The study was approved by National Healthcare Group Domain Specific Review Board E (reference code: 2014/00600) and National University of Singapore Institutional Review Board (reference code: 09–256). The study was carried out in accordance with the principles of the Declaration of Helsinki. All subjects gave written informed consent prior to recruitment. Blood was collected in ethylenediaminetetraacetic acid (EDTA) tubes for flow cytometry and microscopy. Purified PMNs and WB were used for these experiments.

Animals

All mice were bred in the Biological Resource Centre, A*STAR in Singapore. Mice were 8–10 week old females. Breeding pairs for C57BL/6 J (B6) mice were originally obtained from the Jackson Laboratory, ME, US. The derivation of the B6.*Sle1 (Sle1)* and B6.*Sle1Sle2Sle3Sle5* (*Sle123*) congenic mice bearing NZM2410-lupus susceptibility intervals and the generation of the conditional BAC Tg7 have been previously described (28–30). Breeding pairs for all lupus-prone mice were all a kind gift from Prof. Ward Wakeland, UT Southwestern Medical Center, Dallas, TX, US. All mice procedures conformed to National Institutes of Health guidelines and were conducted according to an Institutional Animal Care and Use Committee approved protocol (reference code: 161176).

Blood Sample Collection and Processing

Venous blood from SLE patients and HDs was collected in EDTA tubes. PMNs were purified from WB using Histopaque-1077 (Sigma-Aldrich, MO, US)/Histopaque-1119 (Sigma-Aldrich, MO, US)-based density gradient centrifugation. Briefly, gradients were centrifuged at 400*g* for 30 min at room temperature (RT) without brake and PMNs at the interface between Histopaque-1077 and Histopaque-1119 were collected. Red blood cells were lysed using ACK lysing buffer (Lonza, Basel-Stadt, Switzerland). The PMNs were washed in phosphate buffered saline before being resuspended in RPMI (Gibco, MA, US) supplemented with 10% fetal bovine serum (FBS) and 1% penicillin/streptomycin. PMN purity after density gradient centrifugation was determined using flow cytometry (Supporting Information Table S1). The final cell suspension was typically >95% PMNs.

Murine Bone Marrow Cell Preparation

BM cells were harvested from mouse femurs and tibias. Briefly, after separating the bones, the BM cells were flushed using RPMI onto a 50 ml conical tube through a 70 μm cell strainer. They were then centrifuged at 450 *g* for 5 min at RT and resuspended in RPMI supplemented with 10% FBS and 1% penicillin/streptomycin.

Murine PMN and Platelet Preparation

BM cells were harvested from mouse femurs and tibias as described above. Murine PMNs were purified from BM cells using Histopaque-1077 (Sigma-Aldrich, MO, US)/Histopaque-1119 (Sigma-Aldrich, MO, US)-based density gradient centrifugation. They were then centrifuged at 400*g* for 30 min at RT and resuspended in RPMI supplemented with 10% FBS and 1% penicillin/streptomycin. For platelet (PLT) isolation, peripheral blood was collected via cardiac puncture. Platelet rich plasma was collected after centrifugation (150*g* for 10 min at RT without brake) and washed in Tyrode's buffer containing prostaglandin E1 (1 μM final concentration) (Cayman Chemical, MI, US). The suspension was centrifuged for 150*g*, 10 min at RT without brake to pellet contaminating erythrocytes and leukocytes. The platelet pellet was obtained after centrifugation for 800*g*, 10 min at RT without brake and resuspended in RPMI supplemented with 10% FBS and 1% penicillin/streptomycin.

Measurement of NETosis by Flow Cytometry

For all the following flow cytometry procedures, we maintained a standard operating procedure (SOP) (Supporting Information Table S1). Cells were seeded at a density of 1×10^5/100 μl in U-bottom 96-well polypropylene plates and allowed to adhere for 30 min. Totally 100 μl of PMA (Sigma-Aldrich, MO, US) was then added at the specified concentrations to induce NETosis, or they were left unstimulated. For some experiments, PMNs were incubated with PLTs at various PMN:PLT ratios to induce NETosis. Cells were incubated for up to 4 h at 37°C in 5% CO_2 and fixed by adding 100 μl of 4% paraformaldehyde (PFA; EMS, PA, US) for 15 min at RT. The final concentration of PFA was 1.3%. PFA at concentrations of

1%–4% fix but do not permeate the plasma membrane (21). Following fixation, samples were centrifuged at 100*g* for 10 min at RT. The supernatant was carefully aspirated and 100 µl of a staining master mix was added for 15 min at RT in the dark before analysis by flow cytometry. The master mix consisted of CD66-FITC (BD Pharmingen, NJ, US) or Ly6G-PerCP-Cy5.5 (BD Pharmingen, NJ, US), 0.1 µM SO (Thermo Fisher Scientific, MA, US), and 0.3 nM DAPI (Thermo Fisher Scientific, MA, US) in phosphate buffered saline (PBS; Gibco, MA, US) (Supporting Information Fig. S1A). Final concentrations for CD66-FITC and Ly6G-PerCP-Cy5.5 were 1 µg/ml and 2 µg/ml, respectively. Antibodies and DNA dyes were carefully titrated to negate the need for washing steps since they can disrupt the fragile NET structures (8).

Multiplex Adaptations to the NETosis Protocol

In some cases, additional fluorescent antibodies and often a more complex flow cytometry panel are essential for data analysis. In these cases, we observed increased background fluorescence and therefore removal of unbound antibodies by washing was necessary. Hence, the above protocol was adapted to include washing steps. Following fixation, samples were washed in PBS and centrifuged at 100*g* for 10 min at 4°C without the centrifuge break on. The antibody master mix consisted of CD66b-PerCP-Cy5.5 (BioLegend, CA, US) and NE-Alexa Fluor 488 (Novus Biologicals, CO, US). 100 µl of antibody staining cocktail was added for 30 min at 4°C in the dark. Final concentrations for CD66b-PerCP-Cy5.5 and NE-Alexa Fluor 488 were 1 µg/ml and 13 µg/ml, respectively. After washing in PBS twice, 100 µl of DNA dyes were added as the final step prior to flow cytometric analysis. As SO and DAPI emit fluorescence after binding to DNA, the washing step to remove unbound dye can be omitted (20,31).

Flow Cytometry Acquisition and Analysis

All flow cytometry experiments were performed on a BD FACSCanto II (BD Biosciences, NJ, US) using BD FACSDiva, version 6.1.3 (BD Biosciences, NJ, US) software and analyzed using FlowJo, version 10.4.2 (BD, NJ, US). For the flow cytometry experiments performed on the BD FACSCanto II, the filters for DAPI, FITC and SO were 450/40, 530/30, and 585/42, respectively.

Measurement of NETosis by Immunofluorescence Confocal Microscopy

NETosis was verified using an established fluorescent microscopy protocol with the following modifications (32). Neutrophils were resuspended at 4×10^6 cells/ml RPMI and 250 µl was added to each well of a 12-well plate containing a 15 mm coverslip. An equal volume of PMA was added for 4 h, 37°C, 5% CO_2. Following stimulation, PMNs were fixed using an equal volume of 4% PFA, 15 min, RT. The coverslip was then removed using forceps and placed carefully onto a drop of CD66-FITC for 30 min at 4°C in the dark. The cover slip was washed on PBS drops for 5 min twice before staining with DNA dyes for 15 min, RT. The cover slip was then prepared for microscopy by mounting onto a microscope slide with Fluorescence Mounting Medium (Dako, CA, US). Images were acquired using 10× air objective on Olympus FV1000 or 40× oil objective on Zeiss LSM800 confocal microscopes. For the microscopy experiments performed on the Zeiss LSM800 confocal microscope, the filters for DAPI/ Hoechst 33342, FITC, and SO were SP 470, SP 545, and SP 620, respectively.

Measurement of NETosis by Time-Lapse Live-Cell Immunofluorescence Microscopy

Purified PMNs were stimulated with 30 nM PMA and immediately stained with 1 µg/ml CD66-FITC, 0.2 µg/ml Hoechst 33342 (Thermo Fisher Scientific, MA, US) and 0.1 µM SO. They were analyzed until 4 h poststimulation by confocal live-cell imaging on the Zeiss LSM 710 confocal microscope using a 20× objective. Images were captured every 15 min and analyzed for quantification of NETosis using ImageJ (NIH, MD, US). Calculations were based on >700 PMNs in five different areas. NETosis rate was calculated according to previous descriptions as follows (9):

$$\text{NETosis rate} = 100 \times \textit{Objects counted}\,(\textit{SO channel})/\textit{Objected counted}\,(\textit{Hoechst channel}).$$

Flow Cytometry Assessment of Apoptosis

Apoptosis was induced using etoposide (Sigma-Aldrich, MO, US). PMNs were seeded at a density of 1×10^5/100 µl in U-bottom 96-well polypropylene plates and allowed to adhere for 30 min before being exposed to etoposide (30 µM for 4 h). The PMNs were made to react with annexin V-Alexa Fluor 488 and propidium iodide (Thermo Fisher Scientific, MA, US) according to the manufacturer's instruction.

Statistical Analysis

Data were analyzed using Prism 7.03 (GraphPad Software, CA, US). Normal distribution was assessed using the Shapiro–Wilk test. Gaussian data was analyzed using a Student's *t*-test for two comparisons and one-way ANOVA with post hoc for three or more comparisons and Pearson's correlation coefficient. For time and dose response analyses, a two-way ANOVA was performed with Dunnett's multiple comparison test. Non-parametric data were assessed using Mann–Whitney test for two comparisons and Spearman's rank correlation coefficient. Statistical significance was defined as a two-tailed *P* value of <0.05.

Results

Choice and Titration of Antibodies and Dyes for NETosis Assay Using Flow Cytometry

To optimize a flow cytometry-based assay for NETosis, we began by assessing a series of fluorescently labeled antibodies to distinguish between untreated and PMA-treated human PMNs. We discriminated human PMNs from other possible leukocytes using a combination of antibodies to several cell-surface markers, including CD14, CD16, CD115, CD193, and Siglec-10 (Supporting Information Fig. S1A and data not shown). CD66 antibody was subsequently selected, as

it labels both inactivated and activated PMNs and can be used for both flow cytometry and microscopy (33) (Fig. 1B). CD66 monoclonal antibodies react only with granulocytes and the surface expression of CD66 is upregulated from intracellular stores following stimulation with a wide variety of agents (34). Ly6G was selected to define murine BM-derived PMNs (4).

PMA is a consistent inducer of NETosis in vitro triggering the release of NET-DNA into the extracellular space; a mechanism that requires PMN lysis (35,36). Our strategy was therefore to choose plasma membrane-impermeable DNA dye for the detection of NET-DNA to avoid unspecific labelling of DNA in other forms of cell death. We tested antibodies and DNA dyes previously used in microscopy to label NETs (32,37) (Supporting Information Fig. S1B,C). SO and DAPI were selected as SO does not cross the plasma membrane of live cells and DAPI is membrane-semi-permeable penetrating plasma membranes less efficiently in live cells, making them less susceptible to DAPI-staining (20,38–40). It is thought that PFA at concentrations of 1%–4% can fix but not permeate the plasma membrane to induce artificial "NET formation" (21). On the contrary, we found that the percentage of SO^+DAPI^+ PMNs, depending on the concentrations and exposure duration of PFA, varied on flow cytometry (Supporting Information Fig. S1D,E). For our assays we used a final concentration of 1.3% PFA for 15 min for the detection for extracellular NET-DNA by SO and DAPI. This combination of optimally diluted antibody and DNA dyes identified NETting PMNs with minimal background in fluorescence by confocal microscopy (Fig. 1C).

Gating Strategy to Determine the Percentage of PMNs Undergoing NETosis

Purified PMNs were processed as described above and stimulated with or without PMA. They were then stained with anti-CD66, DAPI and SO, and NETosis were analyzed with flow cytometry using the gating strategy in shown in Figure 2. We initially gated on FSC-A/FSC-H and SSC-A/SSC-H to exclude cell doublets as described in an earlier report (41,42) and observed minimal doublet formation with flow cytometry (Fig. 2A). The cells were then gated on FSC/SSC [region 1 (R1)] to exclude any lymphocyte and monocyte contamination (Fig. 2B). PMNs were then identified based on their high granularity (SSC^{hi}) and surface expression of CD66 (Fig. 2C). Flow cytometry analysis of $SSC^{hi}CD66^+$ PMNs revealed an increase percentage of SO^+DAPI^+ PMNs following PMA treatment (Fig. 2C, D). The background reading for percentage of SO^+DAPI^+ PMNs in untreated samples ranged from 7% to 20%. We observed a decrease in SSC profile and increase in surface expression of CD66 in PMNs following PMA treatment, consistent with the earlier reports (34,42).

Sensitive and Specific Determination of NETs by Flow Cytometry-Based Assay

To assess the sensitivity of our assay, we examined NETosis with lower concentrations of PMA for shorter periods of time. Purified PMNs from five different HDs were stimulated with the indicated concentrations of PMA and analyzed hourly for up to 4 h (Fig. 3A). Using our assay, we observed a significant level of NETosis compared to untreated samples as early

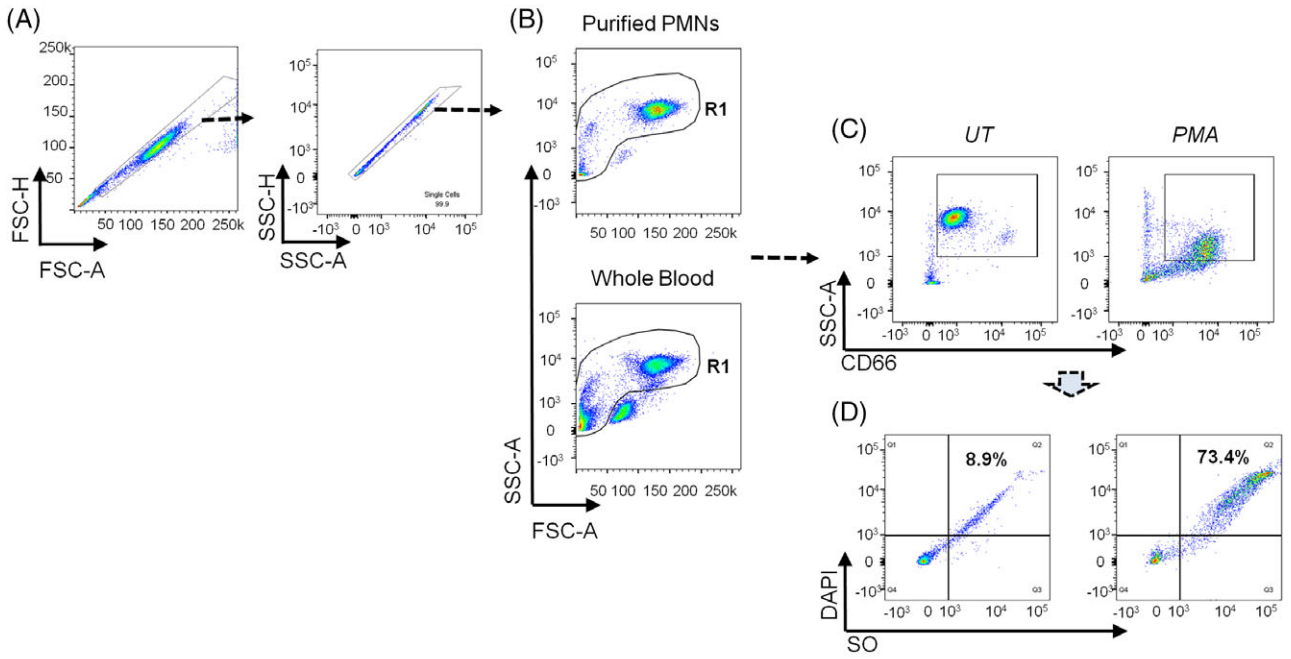

Figure 2. Gating strategy for quantifying NETosis using flow cytometry. (**A**) Single cells were gated using FSC-A/FSC-H and SSC-A/SSC-H. (**B**) Contaminating lymphocytes and monocytes were excluded from analysis by applying R1. (**C**) The PMN population was identified by $SSC^{hi}CD66^+$. (**D**) NET detection by SO and DAPI positivity in untreated and PMA-treated (100 nM) samples.

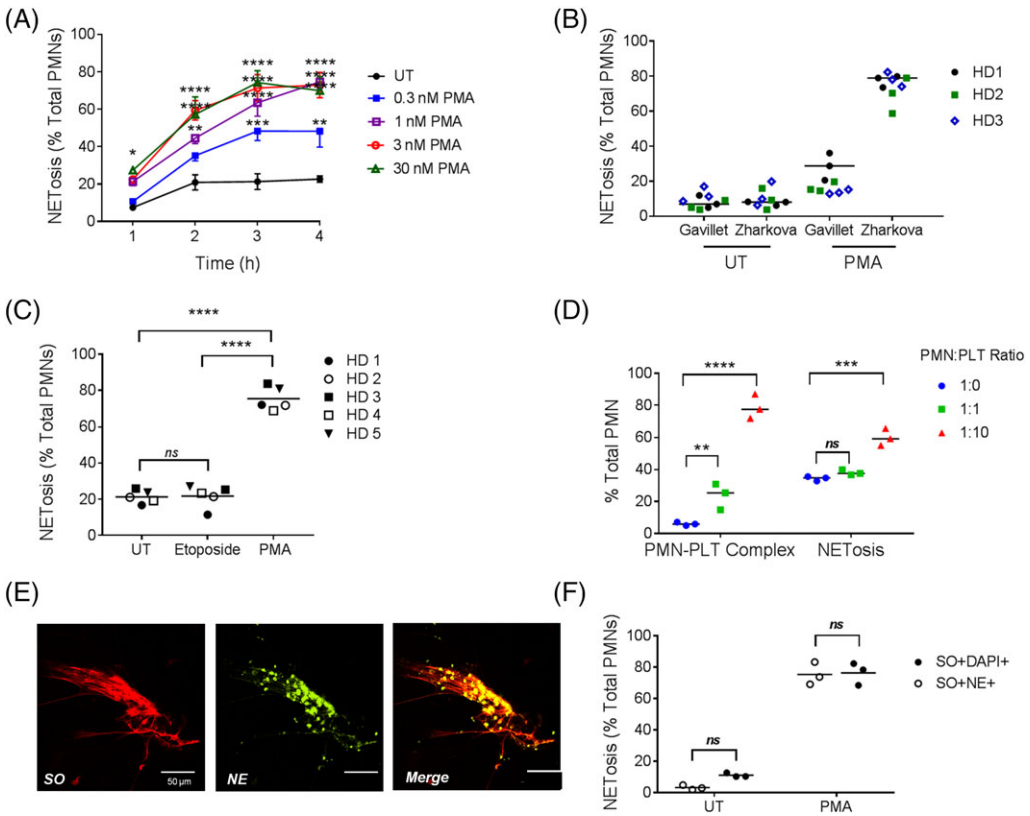

Figure 3. Flow cytometry provides a sensitive and specific assay for detecting NETosis. Purified PMNs were stimulated with different concentrations of PMA as indicated. (**A**) NETosis was detected as early as 1 h following the high concentration of PMA shown and after 3 h with all concentrations used. (**P* < 0.05, ***P* < 0.01, ****P* < 0.001, and *****P* < 0.0001; n = 5). (**B**) PMNs from 3 HDs were untreated or stimulated with PMA (100 nM) for 4 h. The current assay demonstrates improved sensitivity for the detection of NETs compared to a previously published flow cytometry-based assay (22). (**C**) Stimulation with 30 µM etoposide did not result in an increase in SO^+DAPI^+ PMNs. (**ns* = not significant and *****P* < 0.0001; n = 5). (**D**) Isolated BM PMNs and PLTs from B6 mice for incubated at various PMN:PLT ratios (1:0, 1:1, and 1:10) for 3 h. Formation of $SSC^{hi}Ly6G^+CD41^+$ PMN-PLT complexes and NETs were quantified by flow cytometry (**ns* = not significant, ***P* < 0.01, ***P* < 0.001, and *****P* < 0.0001; n = 3). (**E**) Colocalization of NET-DNA and NE in PMA-treated PMNs (100 nM for 4 h). Images were acquired using 40× oil objective on a Zeiss LSM800 confocal microscope. (**F**) Multicolor staining with SO, DAPI, NE-Alexa Fluor 488 and CD66b-PerCP-Cy5.5 was conducted in purified PMNs from HDs, with and without PMA treatment (30 nM for 4 h), before subjecting to flow cytometry (**ns* = not significant; n = 3).

as 1 h following stimulation with the maximum concentration of PMA (30 nM) (Fig. 3A). Lower concentrations (1-30 nM) of PMA reached a significant level of NETosis at 2 h and all concentrations of PMA resulted in significant levels of NETosis at 4 h (Fig. 3A). A comparison with a previously published assay by Gavillet and colleagues revealed a greater sensitivity in the detection of NETosis with our protocol (Fig. 3B and Supporting Information Table S2) (22). To confirm that SO^+DAPI^+ PMNs were recognizing NETosis, we used etoposide to stimulate apoptosis. While annexin V/PI staining showed an increase in early apoptosis at 4 h with 30 µM etoposide (Supporting Information Fig. S1F), there was no increase in the frequency of SO^+DAPI^+ PMNs (Fig. 3C). These findings clearly indicate that SO and DAPI do not recognize early apoptotic PMNs. Previous work has shown that NE binds to DNA and specifically localizes to NETs in a DNA-dependent manner (43). Our immunofluorescent staining confirmed colocalization of NE with DNA fibers extruded from NETting PMNs (Fig. 3E). Furthermore, flow cytometry demonstrated that SO^+DAPI^+ cells were SO^+NE^+ in the PMA-treated PMNs (Fig. 3F). Last, $FSC^{lo}SSC^{lo}Ly6G^-$ dead cells were intermediate SO^+, NETs were SO^+DAPI^+ but dead cells were SO^+DAPI^- (Supporting Information Fig. S2A-C). This may be due to the low concentration of DAPI optimized for our flow cytometry assay detecting only extracellular NETs and not dead cells. Counterstaining dead cells requires 2 µM DAPI for flow cytometry, compared to 0.3 nM DAPI used in this assay (44). Hence, two-color determination using SO and DAPI DNA dyes to detect NET-DNA is required.

Similar results were reproduced by an independent scientist (H.Y. Lee) following the SOP described in Supporting Information Table S1 (Supporting Information Fig. S3A,B).

Comparison of Flow Cytometry-Based Assay with Immunofluorescence Microscopy and Time-Lapse Live-Cell Immunofluorescence Microscopy

Having demonstrated the sensitivity and specificity of the assay for NETosis, we went on to directly compare NETosis measured by microscopy with flow cytometry in the same HDs.

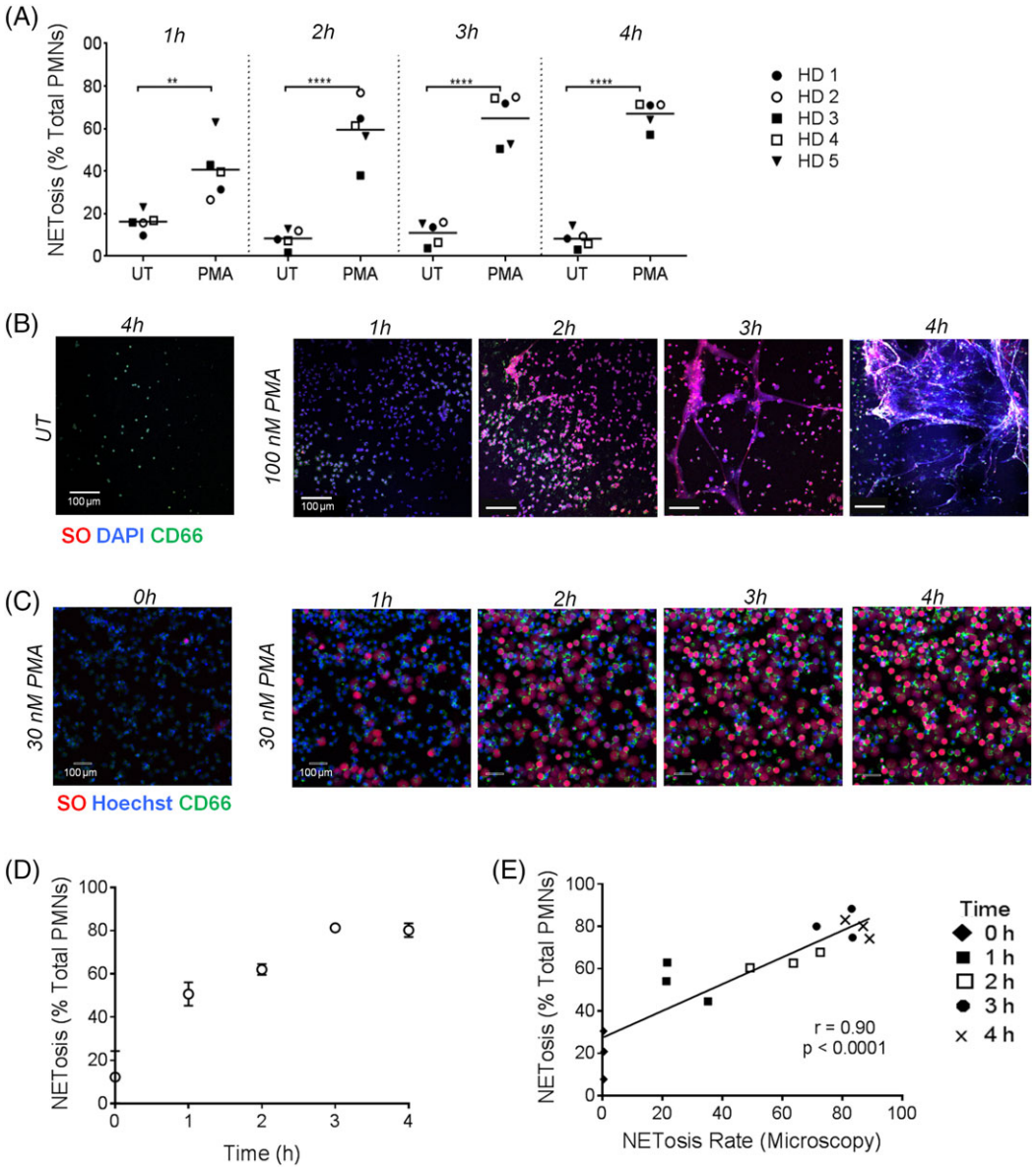

Figure 4. Validation of the flow cytometry assay using microscopy techniques. PMNs were stimulated with PMA and prepared for quantification of NETosis as described. (**A**) NET formation was measured using flow cytometry. Graphs show the percentage of SO^+DAPI^+ PMNs following stimulation with 100 nM PMA every hour from five HDs. (**P < 0.01 and ****P < 0.001; n = 5). (**B**) In parallel, immunofluorescence microscopy was performed to visualize NETs in the same HDs. Representative imaging of UT and PMA-treated PMNs from one of five HDs, acquired every hour. NET-DNA was labeled with SO and DAPI. Images were acquired using 10× objective on Olympus FV1000 confocal microscope. (**C**) PMNs from 1 of 3 HDs were stimulated with 30 nM PMA for 0, 1, 2, 3, and 4 h and monitored using time-lapse live-cell immunofluorescence microscopy. Images were acquired using 20× objective on a Zeiss LSM800 confocal microscope. (**D**) Time course of PMA-induced (30 nM) NETosis of PMNs from one HD, measured in triplicate, using flow cytometry. (**E**) Correlative assessment of levels of NETosis between time-lapse live-cell immunofluorescence microscopy and flow cytometry following PMA (30 nM) exposure at the indicated times. NETosis was measured in PMNs from 3 HDs on the same day (r = 0.90, ****P < 0.001; n = 3).

We stimulated purified PMN with 100 nM PMA and measured NETosis every hour using both methods (Fig. 4A-B). Similar to the increase in the double SO^+DAPI^+ population observed in flow cytometry following PMA exposure (Fig. 4A), NET structures were clearly visualized through colocalization of SO and DAPI (i.e., purple) at 2, 3, and 4 h poststimulation (Fig. 4B).

Hoechst 33342 is a plasma membrane-permeable DNA dye and has been used extensively to stain live cells and therefore may be used as an internal control to quantify total PMN-DNA (DNA in intact PMNs and NETs) and create a ratio of NET-DNA/total PMN-DNA (i.e., NETosis rate) (35,45). We therefore, used time-lapse live-cell immunofluorescence microscopy to determine the NETosis rate following PMA stimulation at the indicated times (Fig. 4C). Similarly, as early as 2 h following PMA stimulation, colocalization of SO with Hoechst 33342 was identified (purple; Fig. 4C and

Supporting Information Video S1). These studies were done in parallel with flow cytometry using SO^+DAPI^+ to identify NETs (Fig. 4D). The NETosis rate obtained using time-lapse live-cell immunofluorescence microscopy exhibited a positive correlation with the percentage of NETting PMNs on flow cytometry (Fig. 4E; $r = 0.90$, $^{****}P < 0.001$).

Additionally, we examined the intraassay variance (PMNs from the same HD in triplicate run on the same day at the same time) and inter-assay variance (PMNs from same HD on three different days) of the flow cytometry assay. The intraassay and interassay variances for the percentage of SO^+DAPI^+ PMNs 4 h poststimulation with 30 nM PMA were 3.98% and 4.66%, respectively.

Detection and Quantification of NETosis within Mixed Cell Populations in SLE Patients and HDs Using Flow Cytometry

All current methods currently used in assessing NETosis involve neutrophil isolation by density centrifugation methods, which may provoke cellular depletion and activation (46). Therefore, an obvious advantage of a new NETosis assay would be the ability to measure function in unseparated cells. We therefore went on to examine NETosis in lysed WB and isolated PMNs in the same donors. We observed a similar frequency of SO^+DAPI^+ NET-appendant PMNs in untreated and PMA-stimulated PMNs across between lysed WB and purified PMN preparations (Fig. 5A). Furthermore, statistical analyses confirmed a positive correlation in NETosis between the two PMN preparations (Fig. 5B; $r = 0.79$, $^{****}P < 0.001$). In summary, our flow cytometry assay permits the study of NETosis in mixed cell populations such as lysed WB, reducing sample manipulation.

Comparison of NETosis in PMNs from SLE Patients and Lupus-Prone Mice with Controls

A previous study reported no differences in NET formation between normal-density PMNs from SLE patients and HDs at baseline or following 2 h stimulation with PMA (47). A comparison of PMA-induced NETosis by flow cytometry in purified PMNs and WB PMNs from SLE patients with HDs did not reveal any significant difference as a result of disease (Fig. 6A,B). However, most of the recruited SLE patients examined were on immunosuppressive therapy with quiescent disease activity, which may have consequences for PMN activation (Supporting Information Table S3). Therefore, we went on to examine NET formation in BM PMNs from young female lupus-prone mice. The NZM2410-derived *Sle1* lupus susceptibility region confers a loss of tolerance to nuclear material, resulting in anti-nuclear antibody titers, increased T and B-cell activation and mild splenomegaly (28,29). The introgression of the additional NZM2410-derived *Sle2* and *Sle3* regions (*Sle123*), or a moderate 2-fold increase in TLR7 (Tg7) results in severe lupus nephritis (48). Stimulation with PMA resulted in an increase in the frequency of SO^+DAPI^+, $SSC^{hi}Ly6G^+$ BM PMNs, which was augmented in *Sle1* mice, compared to B6 controls (Fig. 6C,D). An analysis of BM PMNs across all lupus-prone mice (*Sle1*, *Sle1*Tg7, and *Sle123*) showed an increase in NETosis in severe-lupus prone *Sle123* mice compared to the milder lupus-prone *Sle1* strain (Fig. 6E). Last, the formation of PMN and PLT complexes induced NET formation when BM PMNs and PLTs from B6 mice for incubated at various PMN: PLT ratios (1:0, 1:1, and 1:10) for 3 h (Fig. 3D) (49).

Discussion

In this article, we detailed and validated a novel flow cytometry assay to detect NETs in mixed cell populations using a combination of fluorescently labeled monoclonal antibody against PMN cell-surface markers with DNA dyes (50). NETs are very fragile even after fixation and have to be handled gently, otherwise the majority will get lost during preparation (32). In addition, a common problem with the generation of novel assays is reproducibility by another operator (51,52). We generated a SOP and an independent scientist not involved in the original design of the assay reproduced the findings. Therefore, this flow cytometry assay is simple, reproducible and obviates losses of NETs encountered in the standard methods of analysis.

We validated the assay by showing: (1) minimal SO^+DAPI^+ PMNs with etoposide-induced apoptosis; (2) a positive correlation in the percentage of SO^+DAPI^+ PMNs with NETosis rate obtained using time-lapse live cell microscopy; and (3) colocalization of extracellular DNA and NE on flow

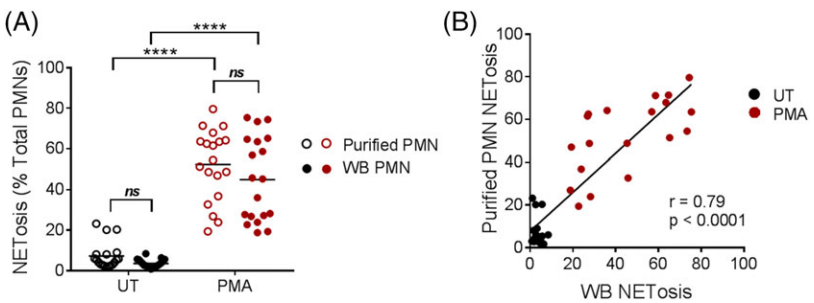

Figure 5. Detection of NETs in mixed cell populations. Flow cytometry assays were performed in each subject with or without isolation of PMNs. (**A**) Cumulative data for percentage of SO^+DAPI^+ PMNs in the total PMN population (either purified PMNs or WB PMNs) from HDs, untreated and stimulated with 30 nM PMA for 4 h (n = 19). (**B**) Correlative assessment of the percentage of NETting PMNs between purified PMNs and WB PMNs in SLE patients and HDs using flow cytometry.

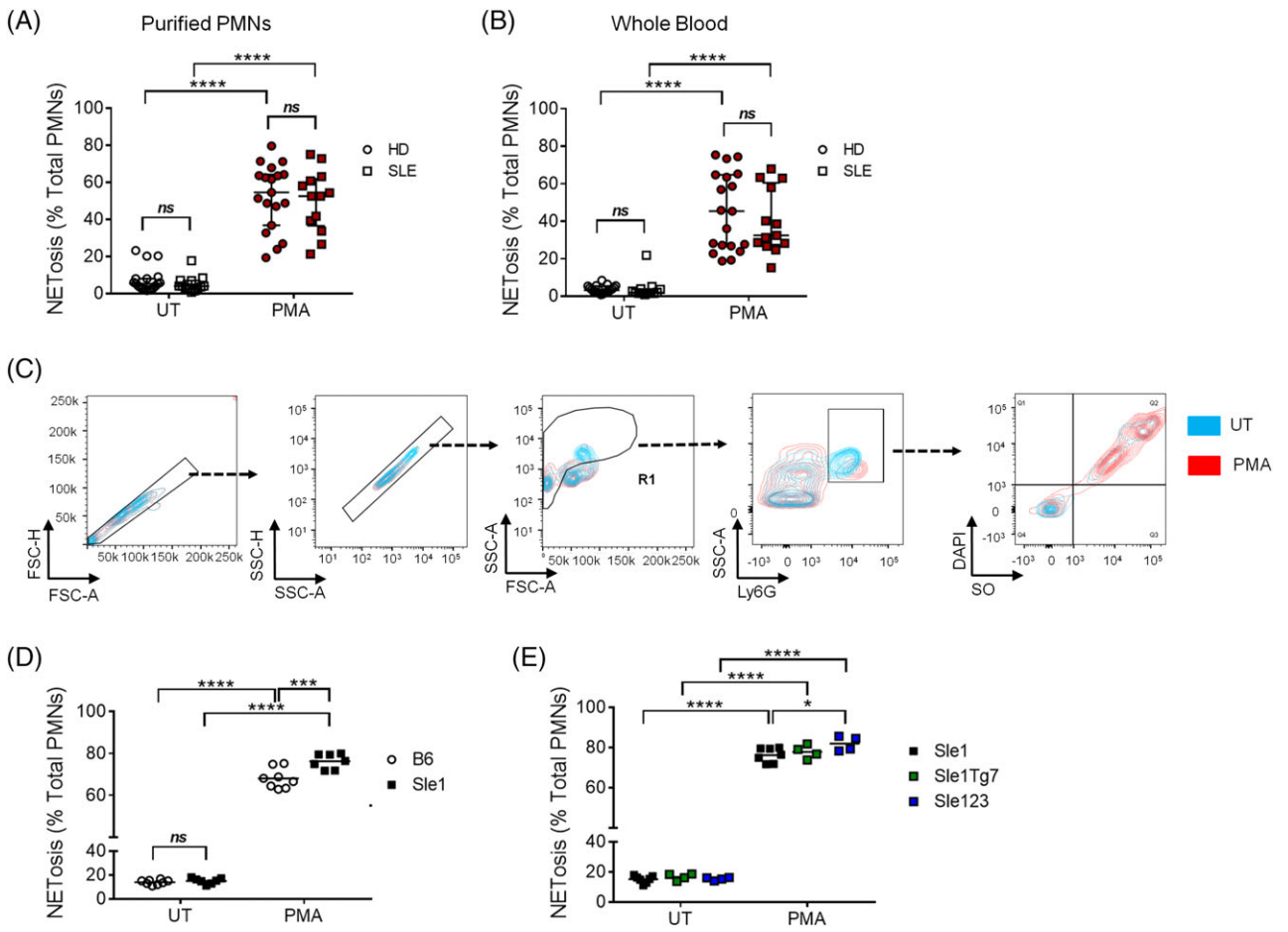

Figure 6. NETosis is increased in murine PMNs from lupus-prone mice. Quantification of NETosis of (**A**) purified PMNs and (**B**) WB PMNs from SLE patients (n = 13) and HDs (n = 19), untreated or exposed to 30 nM PMA for 4 h. The percentage of SO^+DAPI^+ PMNs in the total $CD66^+$ PMN population is shown. A single cell suspension of BM cells from 6 to 8 week old nonautoimmune prone B6 mice (n = 8) or lupus-prone mice [*Sle1* (n = 7), *Sle1*Tg7 (n = 4) and *Sle123* (n = 4)] were stimulated with or without 30 nM PMA for 4 h. NETosis was assessed by flow cytometry. The percentage of SO^+DAPI^+ PMNs in the total in the total $Ly6G^+$ PMN population is shown. (**C**) Flow cytometry gating strategy for measuring NETosis in BM PMNs following stimulation with 30 nM PMA for 4 h, with untreated 4 h as an overlay. BM PMNs are $SSC^{hi}Ly6G^+$. (**D**) A comparison of NETosis in B6 and the mild autoimmune prone strain, *Sle1.* (F) *Sle123* mice which are susceptible to severe autoimmune pathology show increased NETosis compared to *Sle1* mice which have mild autoimmunity.

cytometry. Additionally, we demonstrated that this flow cytometry-based assay could be used for both human and murine samples, in purified PMNs or in mixed cell populations extracted from WB or BM. Moreover, this is the first assay, which does not require purification, which may activate the PMNs (22,24–26).

Over the last few years, a number of flow cytometry-based assays to determine NETs have been proposed (22,24,25). Gavillet et al. described an assay using antibodies against citrullinated H3 and MPO, in combination with DAPI (22). Flow cytometry assays are not expected to detect NETosis from every kind of stimulation since previous data has shown that PAD4-mediated hypercitrullination of histones depends on the nature of the stimulation (21). A side by side comparison with the assay by Gavillet et al. revealed greater sensitivity in the detection of NETosis with our protocol (Fig. 3B and Supporting Information Table S2) (22). Furthermore, Nel et al. identified extracellular NETs as $CD16^-$Vybrant DyeCycle (VDC) $Ruby^+MPO^+$ or $CD16^-$VDC $Ruby^+$citrullniated $H4^+$ (24). VDC Ruby is a plasma membrane-permeable DNA dye (53). However, the assay by Nel et al. can underestimate the earlier phases of NETosis when the NETs are still PMN-appendant. Additionally, Masuda et al. utilized Sytox Green (SG), a plasma membrane-impermeable DNA dye, to detect PMN-appendant NET-DNA (21,25). Similar to our findings, percentage of SG^+ cells correlated with NET area stained using DAPI and observed on fluorescent microscopy (25). However, SG^+ cells were gated solely based on FSC and SSC properties, which limit the assay to purified populations and may include debris (54). To discriminate NETting PMNs from other contaminating leukocytes, a combination of antibodies to other cell-surface lineage markers may be introduced to the flow cytometry panel using our multiplex adaptation described above. As we gated on $SSC^{hi}CD66^+$ or $SSC^{hi}Ly6G^+$ for human and murine PMNs, respectively, and CD66 and Ly6G are well accepted markers for PMNs; this gate should

not have much contamination from other leukocytes. However, we believe a limitation of our assay is underestimating the late phases of NETosis by identifying NETting PMNs as $SSC^{hi}CD66^{+}$ or $SSC^{hi}Ly6G^{+}$, because completely lysed PMNs will fall outside this gate. Hence, we agree that gating based on FSC and SSC is inadequate but cells positive for MPO/NE-DNA complex should be considered as PMNs that have formed NETs (21,25,54). Late apoptotic or necrotic cells induced by etoposide requires incubation for 24 h (55). However, our assay is optimized to avoid spontaneous cell death in neutrophils that may occur with lengthy incubation periods. As such, it is possible that this SO and DAPI will eventually stain late apoptotic and necrotic cells at later time points but that is not the intended use of this assay, where the incubation time was limited to 4 h. The background reading for percentage of $SO^{+}DAPI^{+}$ PMNs in untreated samples ranged from 7% to 20%. This could be due to some loss of integrity as a result of PFA fixation, given the findings we report in Supporting Information Figure S1D comparing PFA concentrations.

Recent evidence suggests that aberrant NETosis and/or impaired NET clearance play a key role in the pathogenesis of SLE (14,47,56). Ribonucleoprotein immune complexes, prevalent in lupus, commit PMNs to NETosis through TLR7/8-mediated shedding of FcγRIIA (57). Furthermore, inhibition of the enzyme, peptidylarginine deiminase 4 (PAD4) blocked NET formation and reduced proteinuria and immune complex deposition in lupus-prone MRL/*lpr* mice (58). PAD4 catalyzes the conversion of arginine residues to citrulline in three of the four histones, H2A, H3 and H4 (10,59). PAD4 is the only PAD that has a nuclear localization signal and is most abundantly expressed in granulocytes, monocytes and mast cells (59). In PAD4-null mice, hypercitrullination of H3 is not detectable and the strain fails to make NETs (3). In apparent contrast to these observations, MRL/*lpr* mice that were deficient in *Nox2*, and therefore lacked functional NADPH oxidase, developed an acceleration of the lupus phenotype (12). However, NADPH oxidase is not the only source of ROS. Mitochondrial ROS production may also generate NETs enriched in oxidized mtDNA, NE, and MPO (12,60). More recently, it has been shown that in addition to PMNs, lymphocytes (B cells, T cells, and NK cells) and monocytes, can release ET-mtDNA (15,16). ET-mtDNA released by B cells was stained with SG and visualized using fluorescence microscopy (16). None of the proteins associated with NETs could be found on B cell ET-mtDNA using mass spectrometry (16). Hence, although ETs classically contain citrullinated histones, MPO and NE; their specific protein composition continues to be defined and varies depending on the source of ETs and disease states (17). As our assay has been optimized for PMN-appendant NET-DNA, it could potentially be adapted to detect and quantify cell-appendant ET-mtDNA from other immune cells.

In conclusion, the assay described here can be easily applied to the flow cytometry study of NETosis for both purified PMNs and mixed cell populations. Analysis of NETosis in the newly described subpopulations of PMNs in WB or BM may open new avenues for researchers in the field (4). Last, high throughput screening for pharmacological inhibitors of aberrant NETosis (e.g., PAD4) may be carried out using our assay as a therapeutic strategy in SLE.

Acknowledgments

The authors wish to express their appreciation to Dr. Bernett Lee of Singapore Immunology Network for statistical support.

Authorship Contributions

O.Z. and S.H.T. designed, performed experiments and analyzed the data; H.Y.L. performed independent experiments; T.S. and W.Y.O. performed the confocal and time-lapse live-cell immunofluorescence microscopy; A.L., P.A.M., L.H.K.L. and J.E.C. provided material and participated in discussions; S.H.T. and A.-M.F. drafted the manuscript; and A.-M.F. oversaw the project.

Disclosure of Conflicts of Interest

The authors declare no competing financial interests.

Literature Cited

1. Brinkmann V, Zychlinsky A. Beneficial suicide: Why neutrophils die to make NETs. Nat Rev Microbiol 2007;5:577–582.
2. Kaplan MJ. Neutrophils in the pathogenesis and manifestations of SLE. Nat Rev Rheumatol 2011;7:691–699.
3. Kuhns DB, Long Priel DA, Chu J, Zarember KA. Isolation and functional analysis of human neutrophils. Curr Protoc Immunol 2015;111:1–16.
4. Evrard M, Kwok IWH, Chong SZ, Teng KWW, Becht E, Chen J, Sieow JL, Penny HL, Ching GC, Devi S, et al. Developmental analysis of bone marrow neutrophils reveals populations specialized in expansion, trafficking, and effector functions. Immunity 2018;48:364–379.e8.
5. Fuchs TA, Abed U, Goosmann C, Hurwitz R, Schulze I, Wahn V, Weinrauch Y, Brinkmann V, Zychlinsky A. Novel cell death program leads to neutrophil extracellular traps. J Cell Biol 2007;176:231–241.
6. Papayannopoulos V, Metzler KD, Hakkim A, Zychlinsky A. Neutrophil elastase and myeloperoxidase regulate the formation of neutrophil extracellular traps. J Cell Biol 2010;191:677–691.
7. Metzler KD, Fuchs TA, Nauseef WM, Reumaux D, Roesler J, Schulze I, Wahn V, Papayannopoulos V, Zychlinsky A. Myeloperoxidase is required for neutrophil extracellular trap formation: Implications for innate immunity. Blood 2011;117:953–959.
8. Brinkmann V, Reichard U, Goosmann C, Fauler B, Uhlemann Y, Weiss DS, Weinrauch Y, Zychlinsky A. Neutrophil extracellular traps kill bacteria. Science 2004; 303:1532–1535.
9. Brinkmann V, Goosmann C, Kuhn LI, Zychlinsky A. Automatic quantification of in vitro NET formation. Front Immunol 2012;3:413.
10. Brinkmann V, Zychlinsky A. Neutrophil extracellular traps: Is immunity the second function of chromatin. J Cell Biol 2012;198:773–783.
11. Goldmann O, Medina E. The expanding world of extracellular traps: Not only neutrophils but much more. Front Immunol 2012;3:420.
12. Lood C, Blanco LP, Purmalek MM, Carmona-Rivera C, De Ravin SS, Smith CK, Malech HL, Ledbetter JA, Elkon KB, Kaplan MJ. Neutrophil extracellular traps enriched in oxidized mitochondrial DNA are interferogenic and contribute to lupus-like disease. Nat Med 2016;22:146–153.
13. Thieblemont N, Wright HL, Edwards SW, Witko-Sarsat V. Human neutrophils in auto-immunity. Semin Immunol 2016;28:159–173.
14. Hakkim A, Furnrohr BG, Amann K, Laube B, Abed UA, Brinkmann V, Herrmann M, Voll RE, Zychlinsky A. Impairment of neutrophil extracellular trap degradation is associated with lupus nephritis. Proc Natl Acad Sci U S A 2010;107:9813–9818.
15. Rocha Arrieta YC, Rojas M, Vasquez G, Lopez J. The lymphocytes stimulation induced DNA release, a phenomenon similar to NETosis. Scand J Immunol 2017;86: 229–238.
16. Ingelsson B, Soderberg D, Strid T, Soderberg A, Bergh AC, Loitto V, Lotfi K, Segelmark M, Spyrou G, Rosen A. Lymphocytes eject interferogenic mitochondrial DNA webs in response to CpG and non-CpG oligodeoxynucleotides of class C. Proc Natl Acad Sci U S A 2018;115:E478–e487.
17. Knight JS, Carmona-Rivera C, Kaplan MJ. Proteins derived from neutrophil extracellular traps may serve as self-antigens and mediate organ damage in autoimmune diseases. Front Immunol 2012;3:380.
18. Yan X, Habbersett RC, Cordek JM, Nolan JP, Yoshida TM, Jett JH, Marrone BL. Development of a mechanism-based, DNA staining protocol using SYTOX orange nucleic acid stain and DNA fragment sizing flow cytometry. Anal Biochem 2000;286: 138–148.

19. Yan X, Habbersett RC, Yoshida TM, Nolan JP, Jett JH, Marrone BL. Probing the kinetics of SYTOX Orange stain binding to double-stranded DNA with implications for DNA analysis. Anal Chem 2005;77:3554–3562.
20. Thermo Fisher Scientific. SYTOX® Orange nucleic acid stain product information. 2001. (accessed on 24 Mar 2018).
21. Masuda S, Nakazawa D, Shida H, Miyoshi A, Kusunoki Y, Tomaru U, Ishizu A. NETosis markers: Quest for specific, objective, and quantitative markers. Clin Chim Acta 2016;459:89–93.
22. Gavillet M, Martinod K, Renella R, Harris C, Shapiro NI, Wagner DD, Williams DA. Flow cytometric assay for direct quantification of neutrophil extracellular traps in blood samples. Am J Hematol 2015;90:1155–1158.
23. Flow cytometric quantification of neutrophil extracellular traps. Limitations of the methodological approach. Am J Hematol 2016;91:965.
24. J GN, Theron AJ, Durandt C, Tintinger GR, Pool R, Mitchell TJ, Feldman C, Anderson R. Pneumolysin activates neutrophil extracellular trap formation. Clin Exp Immunol 2016;184:358–367.
25. Masuda S, Shimizu S, Matsuo J, Nishibata Y, Kusunoki Y, Hattanda F, Shida H, Nakazawa D, Tomaru U, Atsumi T, et al. Measurement of NET formation in vitro and in vivo by flow cytometry. Cytometry A 2017;91:822–829.
26. Jackson MH, Millar AM, Dawes J, Bell D. Neutrophil activation during cell separation procedures. Nucl Med Commun 1989;10:901–904.
27. Hochberg MC. Updating the American College of Rheumatology revised criteria for the classification of systemic lupus erythematosus. Arthritis Rheum 1997;40:1725.
28. Morel L, Mohan C, Yu Y, Croker BP, Tian N, Deng A, Wakeland EK. Functional dissection of systemic lupus erythematosus using congenic mouse strains. J Immunol 1997;158:6019–6028.
29. Morel L, Croker BP, Blenman KR, Mohan C, Huang G, Gilkeson G, Wakeland EK. Genetic reconstitution of systemic lupus erythematosus immunopathology with polycongenic murine strains. Proc Natl Acad Sci U S A 2000;97:6670–6675.
30. Hwang SH, Lee H, Yamamoto M, Jones LA, Dayalan J, Hopkins R, Zhou XJ, Yarovinsky F, Connolly JE, Curotto de Lafaille MA, et al. B cell TLR7 expression drives anti-RNA autoantibody production and exacerbates disease in systemic lupus erythematosus-prone mice. J Immunol 2012;189:5786–5796.
31. Thermo Fisher Scientific. DAPI Nucleic Acid Stain Product Information Volume 2018; 2006.
32. Brinkmann V, Laube B, Abu Abed U, Goosmann C, Zychlinsky A. Neutrophil extracellular traps: How to generate and visualize them. J Vis Exp 2010;36:e1724.
33. Ducker TP, Skubitz KM. Subcellular localization of CD66, CD67, and NCA in human neutrophils. J Leukoc Biol 1992;52:11–16.
34. Skubitz KM, Campbell KD, Skubitz AP. CD66a, CD66b, CD66c, and CD66d each independently stimulate neutrophils. J Leukoc Biol 1996;60:106–117.
35. Carmona-Rivera C, Kaplan MJ. Induction and quantification of NETosis. Curr Protoc Immunol 2016;115:14–41.
36. Phillipson M, Kubes P. The neutrophil in vascular inflammation. Nat Med 2011;17:1381–1390.
37. Akong-Moore K, Chow OA, von Kockritz-Blickwede M, Nizet V. Influences of chloride and hypochlorite on neutrophil extracellular trap formation. PLoS One 2012;7:e42984.
38. Thermo Fisher Scientific. DAPI Product Information. 2018. (accessed on 27 Mar 2018).
39. Scientific TF. Nucleic acid detection and analysis. The Molecular Probes Handbook—A Guide to Fluorescent Probes and Labeling Technologies 2010;11th edition:316.
40. Gomes FM, Ramos IB, Wendt C, Girard-Dias W, De Souza W, Machado EA, Miranda K. New insights into the in situ microscopic visualization and quantification of inorganic polyphosphate stores by 4′,6-diamidino-2-phenylindole (DAPI)-staining. Eur J Histochem 2013;57:e34.
41. Kuonen F, Touvrey C, Laurent J, Ruegg C. Fc block treatment, dead cells exclusion, and cell aggregates discrimination concur to prevent phenotypical artifacts in the analysis of subpopulations of tumor-infiltrating CD11b(+) myelomonocytic cells. Cytometry A 2010;77:1082–1090.
42. Zhao W, Fogg DK, Kaplan MJ. A novel image-based quantitative method for the characterization of NETosis. J Immunol Methods 2015;423:104–110.
43. Thomas MP, Whangbo J, McCrossan G, Deutsch AJ, Martinod K, Walch M, Lieberman J. Leukocyte protease binding to nucleic acids promotes nuclear localization and cleavage of nucleic acid binding proteins. J Immunol 2014;192:5390–5397.
44. Sauvat A, Wang Y, Segura F, Spaggiari S, Muller K, Zhou H, Galluzzi L, Kepp O, Kroemer G. Quantification of cellular viability by automated microscopy and flow cytometry. Oncotarget 2015;6:9467–9475.
45. Thermo Fisher Scientific. Hoechst Stains Product Information Volume 2018; 2005.
46. Alvarez-Larran A, Toll T, Rives S, Estella J. Assessment of neutrophil activation in whole blood by flow cytometry. Clin Lab Haematol 2005;27:41–46.
47. Villanueva E, Yalavarthi S, Berthier CC, Hodgin JB, Khandpur R, Lin AM, Rubin CJ, Zhao W, Olsen SH, Klinker M, et al. Netting neutrophils induce endothelial damage, infiltrate tissues, and expose immunostimulatory molecules in systemic lupus erythematosus. J Immunol 2011;187:538–552.
48. Perry D, Sang A, Yin Y, Zheng YY, Morel L. Murine models of systemic lupus erythematosus. J Biomed Biotechnol 2011;2011:271694, 1, 19.
49. Etulain J, Martinod K, Wong SL, Cifuni SM, Schattner M, Wagner DD. P-selectin promotes neutrophil extracellular trap formation in mice. Blood 2015;126:242–246.
50. Caldwell CW, Taylor HM. A rapid, no-wash technic for immunophenotypic analysis by flow cytometry. Am J Clin Pathol 1986;86:600–607.
51. Manda-Handzlik A, Ciepiela O, Ostafin M, Bystrzycka W, Sieczkowska S, Moskalik A, Demkow U. Flow cytometric quantification of neutrophil extracellular traps: Limitations of the methodological approach. Am J Hematol 2016;91:E9–E10.
52. Naccache PH, Fernandes MJ. Challenges in the characterization of neutrophil extracellular traps: The truth is in the details. Eur J Immunol 2016;46:52–55.
53. Thermo Fisher Scientific. Vybrant DyeCycle ruby stain product information. 2008; (accessed on 1 Apr 2018).
54. Williams DA, Gavillet M. Response to correspondence: Flow cytometric quantification of neutrophil extracellular traps: Limitations of the methodological approach by Ciepiela et al. Am J Hematol 2016;91:E10.
55. Kapiszewska M, Cierniak A, Elas M, Lankoff A. Lifespan of etoposide-treated human neutrophils is affected by antioxidant ability of quercetin. Toxicol In Vitro 2007;21:1020–1030.
56. Denny MF, Yalavarthi S, Zhao W, Thacker SG, Anderson M, Sandy AR, McCune WJ, Kaplan MJ. A distinct subset of proinflammatory neutrophils isolated from patients with systemic lupus erythematosus induces vascular damage and synthesizes type I IFNs. J Immunol 2010;184:3284–3297.
57. Lood C, Arve S, Ledbetter J, Elkon KB. TLR7/8 activation in neutrophils impairs immune complex phagocytosis through shedding of FcgRIIA. J Exp Med 2017;214:2103–2119.
58. Knight JS, Subramanian V, O'Dell AA, Yalavarthi S, Zhao W, Smith CK, Hodgin JB, Thompson PR, Kaplan MJ. Peptidylarginine deiminase inhibition disrupts NET formation and protects against kidney, skin and vascular disease in lupus-prone MRL/lpr mice. Ann Rheum Dis 2015;74:2199–2206.
59. Dwivedi N, Radic M. Citrullination of autoantigens implicates NETosis in the induction of autoimmunity. Ann Rheum Dis 2014;73:483–491.
60. Yousefi S, Mihalache C, Kozlowski E, Schmid I, Simon HU. Viable neutrophils release mitochondrial DNA to form neutrophil extracellular traps. Cell Death Differ 2009;16:1438–1444.